Low Frequency Room Simulation Using Finite Difference Equations

Preprint 4422 (D2)

Søren Krarup Olesen
Aalborg University
Aalborg, Denmark

Presented at the 102nd Convention 1997 March 22–25 Munich, Germany

AN AUDIO ENGINEERING SOCIETY PREPRINT

Low Frequency Room Simulation using Finite Difference Equations

Søren Krarup Olesen

Acoustics Laboratory
Aalborg University, Denmark

Abstract

If the sound transmission in a room is to be simulated at frequencies below about 100 Hz the classic methods of ray-tracing and mirror-imaging are no longer sufficient. Such methods are based on geometrical acoustics that assumes the wave length to be much less than occurring dimensions of the room.

The purpose of this paper is to investigate the method of finite difference equations and compare the result to some measured sound pressures in a test room. The method is attractive for real-time implementation, and in combination with a geometrical model, a wide band room simulation system may be accomplished.

It was found that the method of finite difference equations gave quite good results, however, more exact information about the wall impedances is essential at high frequencies.

0 Introduction

During the last couple of years much attention has been paid to binaural auralisation [1], i.e. the technique of reproducing three-dimensional sound into headphones or loudspeakers, making the listener feel like he or she is in fact present in the intended position. This development gave reason to the term 'virtual reality' (VR) audio, that is, the situation where the listener (user of the VR system) can freely move about in a virtual room, rotate the head and still be able to fix e.g. the position and distance of the sound source and/or feel present in a certain predefined room. Unlike static auralisation, the VR system is capable of updating the filtering in real-time with respect to the users head rotation.

So far, the technique of auralisation (not free field, but including a specific room) only applies to relative high frequencies (above approximately 100 Hz). The head-related transfer functions (HRTF) [2] are perfectly valid at low frequencies, but they are mainly related to plane waves. Plane waves are easily simulated (at high frequencies) using the procedures of ray-tracing or mirror-imaging, and each wave in question can be assigned a certain *direction* from which a proper HRTF should be chosen.

At low frequencies, though, the listener is usually situated in a pressure field which has no direction as such.

Even more important is the fact, that no serious attempt has been made to make a true conjunction between high frequency room simulation and low frequency room simulation. It is usually assumed, that we can create realistic auralisation using geometrical acoustics, and boundary and finite element methods are much to complex and time consuming to deal with anyway—especially when it comes to real-time implementation as required in a VR set-up.

The geometrical methods have been used at low frequencies but only to produce a reliable reverberation time. Doing so, scattering factors were introduced (and found) to distort the intrinsic reflection behaviour of a geometric acoustical simulation, and the correct (measured) reverberation time was finally achieved [3] by adjusting the scattering factors. However, in the light of the complexity of e.g. standing wave phenomenas in rooms it is doubtful, that a convincing transition from geometrical acoustics to low frequency acoustics may be expressed solely by scattering factors.

Another method, that gives us more detailed information about the propagation of sound in rooms at low frequencies, is to describe the whole room and the sound source by means of simple difference equations [4] [5]. The finite difference equation (FDE) method [6] is widely used for numerically solving all sort of differential equation where no explicit solution can be found.

1 The difference equations of linear acoustics

According to the linear inviscid force equation the sound pressure p and the particle velocity $\mathbf{u}$ are related as

$$\nabla p = -\rho \frac{\partial \mathbf{u}}{\partial t} \tag{1}$$

where ρ is the density of the transmission media (usually air, i.e. $\rho \approx 1.21$ kg/m^3). The relation (1) may now be sampled according to time and space using the sampling rates $1/k$ Hz and $1/h$ m^{-1}. A first order approximation of the derivatives can be applied, i.e. a 'straight line' is placed between the two neighbour time/space points in order to estimate the first space derivative of p and the first time derivative of $\mathbf{u}$ at the centre point.

The first order (symmetric) and second order estimation of the first derivative of a function $f(\tau)$ is

$$\frac{\mathrm{d}f(\tau)}{\mathrm{d}\tau} \approx \frac{f(\tau+\Delta\tau) - f(\tau-\Delta\tau)}{2\Delta\tau} \tag{2}$$

Applying (2) on (1) in time and space domain gives us (e.g. in the x-direction) a discrete version of (1) being

$$\frac{p_{x+h,y,z}(t) - p_{x-h,y,z}(t)}{2h} = -\rho \frac{u^x_{x,y,z}(t+k) - u^x_{x,y,z}(t-k)}{2k} \tag{3}$$

where h is the spacious grid size and k is the time-step size. (3) is reduced and time-shifted $-k$ into

$$u^x_{x,y,z}(t) = u^x_{x,y,z}(t-2k) + \frac{k}{\rho h}\left[p_{x-h,y,z}(t-k) - p_{x+h,y,z}(t-k)\right] \wedge$$
$$u^y_{x,y,z}(t) = u^y_{x,y,z}(t-2k) + \frac{k}{\rho h}\left[p_{x,y-h,z}(t-k) - p_{x,y+h,z}(t-k)\right] \wedge$$
$$u^z_{x,y,z}(t) = u^z_{x,y,z}(t-2k) + \frac{k}{\rho h}\left[p_{x,y,z-h}(t-k) - p_{x,y,z+h}(t-k)\right] \quad (4)$$

where u^x, u^y and u^z are the x, y and z components of $\mathbf{u}$.

Yet another relation (the equation of continuity) between sound pressure p and particle velocity $\mathbf{u}$ exists:

$$\text{div } \mathbf{u} = -\frac{1}{c^2\rho}\frac{\partial p}{\partial t} \quad (5)$$

where c is the wave propagation speed. Again we discretise, and sample (5) according to time and space. Applying (2) on (5) yields

$$\frac{u^x_{x+h,y,z}(t) - u^x_{x-h,y,z}(t)}{2h} + \frac{u^y_{x,y+h,z}(t) - u^y_{x,y-h,z}(t)}{2h} + \frac{u^z_{x,y,z+h}(t) - u^z_{x,y,z-h}(t)}{2h} =$$
$$-\frac{1}{c^2\rho}\frac{p_{x,y,z}(t+k) - p_{x,y,z}(t-k)}{2k} \quad (6)$$

which is reduced and time-shifted $-k$ into

$$p_{x,y,z}(t) = p_{x,y,z}(t-2k) + \frac{c^2\rho k}{h}\left[u^x_{x-h,y,z}(t-k) - u^x_{x+h,y,z}(t-k) +\right.$$
$$\left. u^y_{x,y-h,z}(t-k) - u^y_{x,y+h,z}(t-k) + u^z_{x,y,z-h}(t-k) - u^z_{x,y,z+h}(t-k)\right] \quad (7)$$

Formula (4) and (7) can now be used for updating the particle velocity and secondly the sound pressure. One might also have discretised the wave equation directly. The reason for the separation above is that the boundary conditions and sound source are most easily modelled using the particle velocity in each direction x, y and z, i.e. the directional information would be 'hidden' in a plain scalar wave equation description.

2 Boundary conditions

Since the derivative estimation of (2) requires knowledge of the 'next' or 'prior' point in space, we cannot use it when the point in space (x,y,z) lies just next to the wall. Hence we use the following first order (asymmetric) estimation of the first derivative of a function $f(\tau)$ e.g. in the x-direction assuming a wall just right to the point in question:

$$\frac{df(\tau)}{d\tau} \approx \frac{f(\tau) - f(\tau - \Delta\tau)}{\Delta\tau} \tag{8}$$

In fact we get two version of each of the equations (4). Assuming the example just mentioned and applying (8) and (2) on (1) we get one of the six:

$$u^{x}_{x,y,z}(t) = u^{x}_{x,y,z}(t-2k) + \frac{2k}{\rho h}\left[p_{x-h,y,z}(t-k) - p_{x,y,z}(t-k)\right] \tag{9}$$

The last term in (9) is unknown but since u^x represents the perpendicular part of **u** to a right-hand wall, p can be expressed from the characteristic wall impedance Z, and we have

$$u^{x}_{x,y,z}(t) = u^{x}_{x,y,z}(t-2k) + \frac{2k}{\rho h}\left[p_{x-h,y,z}(t-k) - Zu^{x}_{x,y,z}(t-k)\right] \tag{10}$$

where Z is assumed to be real. This assumption is made because only in a few cases we have knowledge about the complex impedance of a certain wall material; common data are rather real absorption coefficients or likewise. Furthermore, the real part of most wall material impedances are in fact the predominate part and Z can then be approximated by

$$Z = \rho c \frac{1+\sqrt{1-\alpha}}{1-\sqrt{1-\alpha}} \tag{11}$$

where α is the absorption coefficient.

The impedance Z goes towards infinity when α becomes very small, thus (10) becomes rather unwieldy. This can be dealt with by assuming that

$$u^{x}_{x,y,z}(t-k) \approx \frac{u^{x}_{x,y,z}(t) + u^{x}_{x,y,z}(t-2k)}{2} \tag{12}$$

Inserting (12) in (10) yields

$$\boxed{u^{x}_{x,y,z}(t) = \frac{\frac{\rho h}{k} - Z}{\frac{\rho h}{k} + Z} u^{x}_{x,y,z}(t-2k) + \frac{2}{\frac{\rho h}{k} + Z} p_{x-h,y,z}(t-k)} \tag{13}$$

When Z approaches infinity, the p quantity vanishes and u depends only of an old value of u. Since the particle velocity is zero to begin with u remains zero, which is perfectly true for fully rigid walls.

Other consideration about (13) could be made; if we choose h=kc and let Z=ρc (full absorption) the boundary condition would then be

$$u^x_{x,y,z}(t) = \frac{1}{\rho c} p_{x-h,y,z}(t-k) \tag{14}$$

In other words; the particle velocity in a point close to an anechoic wall equals the former particle velocity in the perpendicular neighbour point.

The idea of making $h=kc$ simplifies (4) , (7) and (13) in general. It also assures that no space aliasing takes place, however, the sampling frequency $1/k$ should of course be much larger than the test frequency in order to avoid time aliasing.

Since **u** and p is always available during this time domain procedure, any other quantities like the velocity potential ϕ, the intensity **I** and the acoustic power w may be revealed concurrently and used for further analysis.

3 The sound source

The sound source should be defined as a volume velocity occupying one or more points in space depending on the extent of the sound source.

If the sound source is a membrane producing sound velocity in, say the x-direction, the particle velocity in the y- and z-direction should be left untouched and only influenced by the wave equation (4) and (7). If the membrane is rotated the particle velocity is expressed as a fraction between the co-ordinates according to the nature of the rotation.

4 Comparison between the model and a real-life situation

The method of FDE was tested in the following way: A standard listening room was chosen (at the Acoustics Laboratory of Aalborg University). This room has formerly been measured and simulated at low frequencies by Cherek and Langvad [7]. The room size is x=4.13 m, y=7.80 m and z=2.76 m. A loudspeaker is placed at position x=0.30 m, y=7.80 m and z=1.25 m, i.e. inside the front wall when looking in the y-direction. The loudspeaker is an 8" Vifa D25AG35-06 unit fixed in a closed 150 l box. The room was divided into a grid of 60×60 cm^2 (7×13 boxes), and only the sound pressures in the horizontal positions z=1.25 m were measured. In the simulation a dividing of $15 \times 15 \times 15$ cm^3 ($29 \times 53 \times 19$ boxes) was made with the loudspeaker positioned in height of the 8th box.

The measurements were carried out at 20, 40 and 60 Hz controlled by a B&O RC-oscillator TG8 amplified by a Pioneer A-616 reference stereo amplifier, and directly fed to the loudspeaker.

In the middle of each of the 91 boxes a 1" B&K 4144 pressure microphone together with a B&K 2639 pre-amplifier was placed. The precision of microphone placing was within ± 5 cm. Output was fed to a B&K 2636 measuring amplifier and displayed on a Fluke 37 multimeter. The B&K 2636 was set to 1 second averaging time to produce a fairly stable RMS voltage value.

The whole set-up was calibrated using a B&K 4220 pistonphone that produced a sound pressure level of 124 dB at 250 Hz.

The volume velocity of the loudspeaker was unknown, however, the following voltages (RMS) was used; 2.0 V (20 Hz), 1.5 V (40 Hz) and 1.0 V (60 Hz) to feed the loudspeaker.

During the simulation, the floor and each of the walls were assumed to have an absorption coefficient of α=0.1. The ceiling is rather complex, being 'curved' in the corners and of two solid layers: Thin plate, air and finally concrete. An absorption coefficient of α=0.75 was used.

In figure 1 we see in the left column the measured sound pressure levels and in the right column we see the corresponding simulated figures at 20, 40 and 60 Hz accordingly. The SPL's shown in the case of the measured values were actually present in the room during the tone excitement. The SPL's in the simulated case were scaled by a constant to minimise the difference between measurement and simulation.

By the first glance at figure 1 there is no doubt that the main structures of the sound pressure distribution were maintained in the simulation. The results of the simulation gave pronounced patterns of pressure while the measurements gave more blurred values—in particular at 60 Hz. However, the slight bending of the low pressure cleft at 40 Hz was perfectly retained in the simulation. The pressure in close proximity to the loudspeaker is clearly underestimated in the simulation.

5 Discussion

The comparison between the FDE method and actual real-life sound pressures suggested that the FDE method indeed is very useful to predict the sound field in rooms. However, it is vital to know the volume velocity to achieve absolute values.

The divergence, especially seen at 60 Hz, is expected to be due to lack of exact information on the wall impedances, thus, at relative high frequencies a good approximation of the wall impedances involved should be available.

The simplicity of the difference equations (1st or 2nd order) makes them fit for implementation on a digital signal processor (DSP). Such an implementation should be fed directly from the anechoic, lowpass filtered source signal. An auralisation could then be achieved just from tapping the signal from the grid point desired, i.e. the grid point that corresponds to the position of the listener.

One of the most attractive features of the FDE is, that the geometric discretisation of the room should may be set equal to that of the integer based ray-tracing technique described by Olesen [8] [9]. That particular merger is obvious in order to form a complete high-speed wide band room simulation system and in order to assemble data needed for the geometrical description of a room.

References

[1] Mendel Kleiner, Bengt-Inge Dalenbäck and Peter Svensson, Auralization—An overview, *J. Audio Engineering Society*, 41 (11), 1993, pp. 861-875.

[2] Henrik Møller, Mickael Friis Sørensen, Dorte Hammershøi and Clemen Boje Jensen, Head-related transfer functions of human subjects, *J. Audio Engineering Society*, 43 (5), 1995, pp. 300-321.

[3] Jens Holger Rindel and Claus Lynge Christensen, Scattering as a key to improved room acoustic computer modelling, *Proceedings of Nordic Acoustical Meeting*, Helsinki, Finland, 1996, pp. 517.

[4] Lauri Savioja, Timo J. Rinne and Tapio Takala, Simulation of room acoustics with a 3-D finite difference mesh. *Proceedings of International Computer Music Conference ICMC '94*, pp. 463-466.

[5] Dick Botteldooren, Finite-difference time-domain simulation of low-frequency room acoustic problems, *J. Acoustical Society of America*, 98 (6), 1995, pp. 3302-3308.

[6] Walter G. Kelley and Allan C. Peterson, *Difference equations*, Academic Press, London, 1991.

[7] Bogdan Cherek and Bjarne Langvad, Low frequency simulation of a listening room, *Proceedings of Nordic Acoustical Meeting*, Luleå, Sweden, 1990, pp. 265-270.

[8] Søren Krarup Olesen, An integer based ray-tracing algorithm, *Proceedings of 100th Audio Engineering Society Convention*, Copenhagen, Denmark, 1996, preprint 4227, pp. 1-6.

[9] Søren Krarup Olesen, Room simulation: A high-speed model for virtual reality audio systems, *Proceedings of Nordic Acoustical Meeting*, Helsinki, Finland, 1996, pp. 339-342.

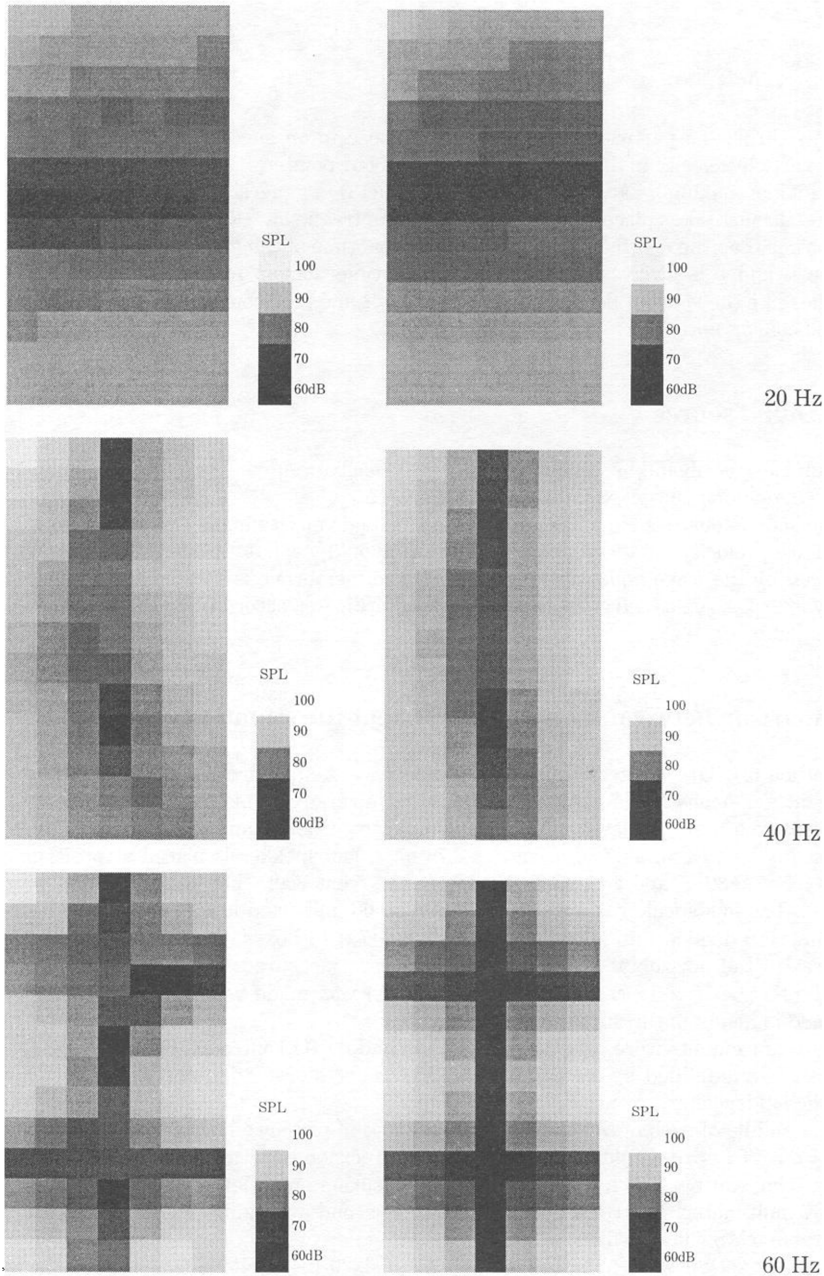

Figure 1. The left column shows the measure sound pressure levels in the test room, and the right column shows the SPL's simulated. The membrane of the sound source is placed on the upper edge of the upper left box in all figures.